Earthquake Engineering & Structural Dynamics
The Journal of the International Association for Earthquake Engineering

EARTHQUAKE ENGINEERING & STRUCTURAL DYNAMICS
Earthquake Engng Struct. Dyn. (2015)
Published online in Wiley Online Library (wileyonlinelibrary.com). DOI: 10.1002/eqe.2609

An analytical model of a deformable cantilever structure rocking on a rigid surface: experimental validation

Rico Truniger, Michalis F. Vassiliou*,† and Božidar Stojadinović

Institute of Structural Engineering (IBK), Swiss Federal Institute of Technology (ETHZ), Stefano-Franscini-Platz 5, 8093 Zürich, Switzerland

SUMMARY

This paper describes an experimental program to examine the dynamic response of deformable cantilevers rocking on a rigid surface. The primary goal of the tests is to verify and validate a dynamic rocking model that describes the behavior of these structures. The benchmark response data was obtained from shaking-table tests on deformable rocking specimens with different natural vibration frequencies and different aspect ratios excited by analytical pulses and recorded ground motions. The responses computed using the model are found to be in good agreement with the benchmark test results. Widely used impact, restitution and damping assumptions are revisited based on the experiment results and the analytical model findings.

Received 24 October 2014; Revised 26 March 2015; Accepted 26 June 2015

KEY WORDS: seismic isolation; seismic modification; rocking; uplifting structures; earthquake engineering; overturning

1. INTRODUCTION

Designing structures with safety factors against uplift smaller than one has been proposed as an earthquake response modification technique. The technique is based on the fact that comparatively large and sustained forces are needed to overturn physically large structures meaning, in turn, that such structures are difficult to overturn by naturally occurring dynamic excitations. While many theoretical models for rocking of rigid structures have been published, there are relatively few theoretical models for rocking of structures whose deformability cannot be neglected. Moreover, even fewer tests have been performed to experimentally examine the behavior of rocking structures [1–8]. These tests have shown that the response and, in particular, the energy dissipation mechanisms of a rocking structure are more complex than typically assumed.

This paper describes a series of experiments that were performed to validate an analytical model for rocking of deformable cantilever structures with massive columns and concentrated masses at the base and the top of the cantilever developed in a companion paper [9]. Specimens with four different fundamental vibration frequencies were mounted on two different uplifting bases and excited by analytical pulses and real ground motions using a shaking table. The observations from the initial tests were used to examine the loss of energy during impact and to propose a new way to analytically model this phenomenon. A description of the tests and the obtained test data is available in [10]. The data can be used to assess other models for uplifting and rocking response of deformable cantilever structures.

*Correspondence to: Michalis F. Vassiliou, Institute of Structural Engineering (IBK), Swiss Federal Institute of Technology (ETHZ), Stefano-Franscini-Platz 5, 8093 Zürich, Switzerland.
†E-mail: mfvassiliou@gmail.com

2. SPECIMENS AND TEST SETUP

A specimen consists of a steel base plate, two columns made using steel threaded rods, and a steel weight at the top (Figure 1, Table I). The configuration of the specimen is deliberately similar to the configuration of the model of a deformable rocking column utilized in the companion paper [9]. The top weight and the base plates are attached to the columns using threaded holes and nuts. Two horizontal stiffeners were mounted between the two columns, as shown in Figure 1, to increase the out-of plane horizontal stiffness and, thus, impede out-of-plane movement.

Four different column diameters are used to make specimens with fixed-base natural frequencies of approximately 1, 2, 3 and 4 Hz. In addition, base plates with widths, b_b, of 15 and 30 cm were used to investigate the influence of the specimen slenderness on the response. The four frequencies and two base plate widths give eight different specimens. Dimensions and masses, together with values of the slenderness α and rocking parameter p [9] as well as the measured fixed-base natural frequencies and damping ratios of the eight specimens, are listed in Table I. The column diameter, d_c, corresponds to the outside diameter of the threaded rod, while the mass m_c includes the two columns, two horizontal stiffeners and the nuts to mount them. The top weight consists of two individual plates. The mass of the top weight, m_w, also includes the mass of the nuts needed to attach the plates to the columns and the mass of a small additional weight placed eccentrically on the top of each specimen to balance it and compensate for the unavoidable manufacturing eccentricity. The fixed-base vibration characteristics were determined in 60-s long free vibration tests. The natural frequencies, f, of the 1, 2 and 3-Hz specimens are independent of the base plate. There is, however, a considerable difference between the measured frequencies of the 4 Hz specimens with the long and the short base plates. An extra 1 kg mass was attached at the top of the 4 Hz Long Base specimen to balance it: this added mass can partly explain the difference in the

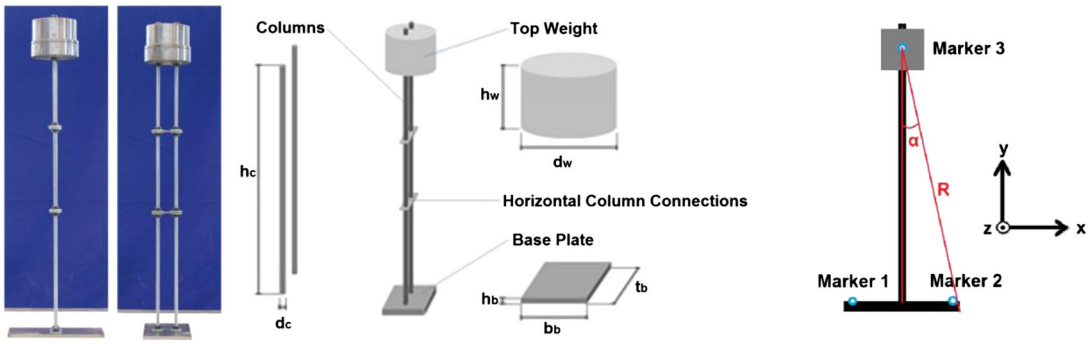

Figure 1. Left: two views of the 4 Hz Long Base specimen. Middle: sketch of a specimen and its components. Right: placement of the infrared markers.

Table I. Dimensions, masses and vibration characteristics of the eight specimens.

Specimen	Vibration char.		Top weight			Column			Base plate				Rocking parameters	
	f_{fix} [Hz]	ζ [%]	h_w [mm]	d_w [mm]	m_w [kg]	h_c [mm]	d_c [mm]	m_c [kg]	h_b [mm]	b_b [mm]	t_b [mm]	m_b [kg]	α [ ]	p [Hz]
1 Hz Long Base	0.94	0.26	125	145	14.72	1000	12	1.75	10	300	150	3.53	0.159	3.22
1 Hz Short Base	1.00	0.16	125	145	14.72	1000	12	1.75	10	150	150	1.77	0.081	3.24
2 Hz Long Base	2.07	0.28	125	145	14.96	1000	16	2.98	10	300	150	3.53	0.160	3.23
2 Hz Short Base	2.05	0.40	125	145	14.96	1000	16	2.98	10	150	150	1.77	0.081	3.25
3 Hz Long Base	3.11	0.60	125	145	15.16	1000	20	4.32	10	300	150	3.53	0.161	3.24
3 Hz Short Base	3.12	0.35	125	145	15.16	1000	20	4.32	10	150	150	1.77	0.081	3.25
4 Hz Long Base	3.84	1.32	125	145	16.65	1000	24	6.34	10	300	150	3.53	0.161	3.24
4 Hz Short Base	4.34	0.76	125	145	15.58	1000	24	6.34	10	150	150	1.77	0.081	3.26

DOI: 10.1002/eqe

measured vibration periods. The damping ratio ζ changed during the free vibration test: the value given in Table I is an average over the first 20 s of the test. Unexpectedly, the damping ratio depends on the base plate width, being smaller for the short base specimens (except for the 2 Hz case).

2.1. *Specimen excitation and the shaking table*

The rocking response of a specimen was induced by dynamics excitation of its support. This was achieved by placing the specimens, one at the time, on the top of the ETH shaking table [11] steel platform. The shaking table platform is a stiff steel box. It is placed on roller bearings and actuated using servo-hydraulic actuators to move only in one horizontal direction. The stroke of the table is 250 mm, and the maximum velocity is 225 mm/s.

Each specimen was tested using 15 different symmetric Ricker wavelets, 12 different antisymmetric Ricker wavelets and 3 earthquake records. A total of 240 tests were conducted.

A Ricker wavelet approximates the main pulse of pulse-type ground motions [12]. Typical symmetric and antisymmetric Ricker wavelets are shown in Figure 2. The acceleration amplitude, a_p, and period, T_p, of a Ricker wavelet are discussed further in [13]. The Ricker wavelets used in this study had the pulse periods T_p ranging from 0.25 s to 2 s and the acceleration amplitudes a_p ranging from 0.04 g to 0.64 g. The values, normalized using the slenderness and the rocking parameter values of the short and long base specimens, are shown in the rocking spectrum plots in Figure 2. The lines shown in the rocking spectrum plots represent the maximum pulse velocity that can be applied by the ETH shaking table for the short and the long base specimens. While the selected specimens and wavelet excitations covered the spectrum parameter space well, it is clear that the maximum table velocity limited the range of rocking response that could be investigated. For example, the 4 Hz short base specimen can rock and overturn in both directions, while the 1 Hz Long Base specimen can rock, but cannot overturn (Figure 2).

Three different earthquake records were used to excite the specimens (Table II). The records were also scaled down because of the limited maximum velocity of the shake table, but were still sufficiently strong to induce rocking in all and overturn some of the specimens.

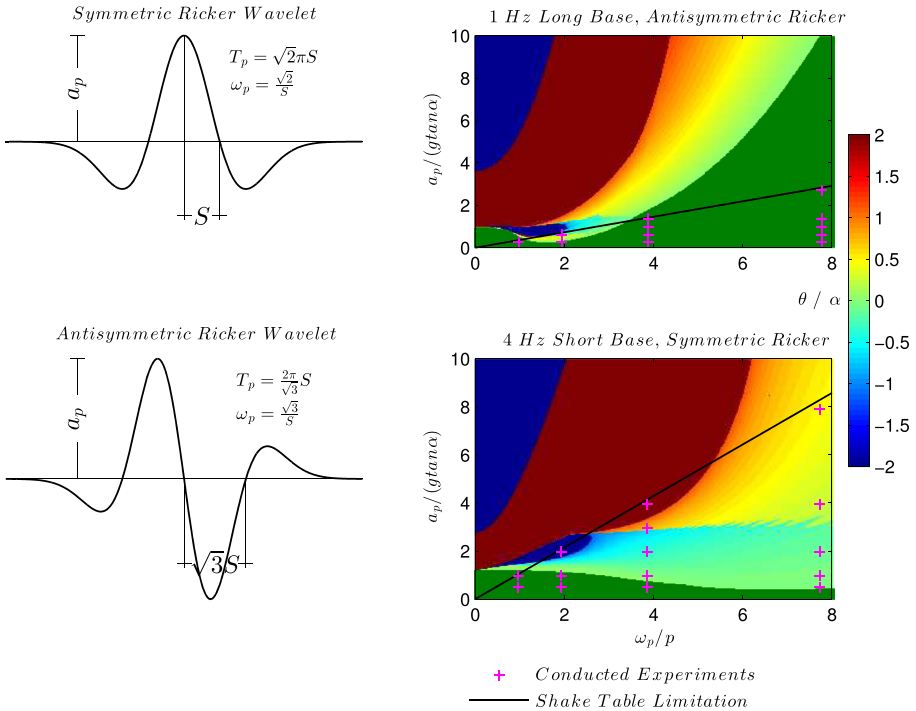

Figure 2. Symmetric and antisymmetric Ricker wavelets and the rocking spectra showing the tested cases and the pulse velocity limit imposed by the ETH shaking table.

DOI: 10.1002/eqe

Table II. Earthquake records used in the tests.

Earthquake	Record station	Source	Magnitude (Mw)	Distance (km)	PGA (g)	PGV (m/s)	a_p (g)	T_p (s)	Scale factor
1971 San Fernando	Pacoima Dam 164	PEER	6.6	11.9	1.23	1.13	0.30	1.35	0.102
1992 Erzican,	Erzincan/NS	PEER	6.9	13	0.52	0.84	0.32	2.00	0.205
1995 Aigio	OTE Building/FN	ITSAK	6.2	20	0.50	0.43	0.44	0.60	0.407

2.2. *Test method*

A layer of sandpaper was taped on the shake table platform to increase the friction between the platform and the specimen base plate with the goal to minimize sliding and stepping of the specimens during the rocking motion. To prevent damage in case of overturning, the top weight of the specimen was connected to the hook of the overhead crane with a loose light string that was neither heavy nor tight enough to affect the response. Motion of the specimens was recorded for 20 to 30 s after the start of the Ricker wavelet excitations, and for 60 s after the start of the earthquake excitations.

2.3. *Data acquisition system*

An Optotrak Certus System, manufactured by Northern Digital Inc., was used to track the position of the specimens during the tests. This system uses active infrared-emitting diodes as markers and a trinocular camera system to determine the position of the markers. Three markers were placed on the specimen to measure its position (Figure 1, right): two markers placed on the base plate were used to determine the rocking angle; the third marker, placed at the center of the top weight was used to measure the elastic deformation of the column and the motion of the top of the specimen. A fourth marker was placed on the shaking table. The accuracy of the system was determined by measuring the position of a marker at rest over a long period of time. In the x- and y-directions in the plane where rocking motion takes place, the accuracy was about 0.02 mm. In the z-direction, perpendicular to the plane of motion, the accuracy was about 0.10 mm.

The position sampling frequency was 500 Hz. The highest measured uplifted vibration frequency was 34 Hz, which means that at least 15 position measurements per marker were taken during an oscillation in the uplifted state of a specimen. This is sufficient to capture the motion of the specimen and measure its frequency. However, assessment of the damping ratio using the logarithmic decrement methods is sensitive to the exact measurement of the amplitude and was, thus, less accurate. This could be one of the reasons for the consistent difference in damping ratios for the long and the short base specimens (Table I).

3. EXPERIMENT OUTCOMES AND OBSERVATIONS

The objective of the experimental campaign was to investigate the rocking response of a deformable column with distributed mass and concentrated masses on its top and its base. Therefore, the tests where the rocking angle amplitudes exceeded 10% of the specimen slenderness (0.1α) are considered in detail, while the tests without uplift or with overturning are used only to verify the rocking spectra. Table III lists the 64 tests with Ricker wavelets where there was uplift but no overturning, and the rocking angle amplitude exceeded 0.1α. The tests are numbered for reference. The results of the earthquake excitation tests are shown separately in a later section.

Typical test response is one where the specimen uplifts and rocks without overturning, without rotation about its vertical axis (twisting), out-of-plane motion, or stepping or sliding on the rocking surface. The following deviations in specimen response were observed:

DOI: 10.1002/eqe

Table III. List of tests with a Ricker wavelet excitation and measured rocking angle amplitudes larger than 0.1α.

No.	Specimen configuration	Excitation type	T_p [s]	a_p [g]
1	1 Hz Long Base	Antisymmetric Ricker	1.00	0.10
2		Symmetric Ricker	1.00	0.08
3		Symmetric Ricker	1.00	0.16
4		Symmetric Ricker	0.50	0.32
5	1 Hz Short Base	Antisymmetric Ricker	1.00	0.04
6		Antisymmetric Ricker	1.00	0.10
7		Antisymmetric Ricker	0.50	0.16
8		Antisymmetric Ricker	0.50	0.22
9		Symmetric Ricker	1.00	0.04
10		Symmetric Ricker	1.00	0.08
11		Symmetric Ricker	0.50	0.16
12		Symmetric Ricker	0.50	0.24
13		Symmetric Ricker	0.50	0.32
14	2 Hz Long Base	Antisymmetric Ricker	0.50	0.10
15		Antisymmetric Ricker	0.50	0.16
16		Antisymmetric Ricker	0.50	0.22
17		Symmetric Ricker	1.00	0.16
18		Symmetric Ricker	0.50	0.16
19		Symmetric Ricker	0.50	0.24
20		Symmetric Ricker	0.50	0.32
21		Symmetric Ricker	0.25	0.64
22	2 Hz Short Base	Antisymmetric Ricker	0.50	0.10
23		Antisymmetric Ricker	0.50	0.16
24		Antisymmetric Ricker	0.50	0.22
25		Antisymmetric Ricker	0.25	0.44
26		Symmetric Ricker	1.00	0.08
27		Symmetric Ricker	0.50	0.08
28		Symmetric Ricker	0.50	0.16
29		Symmetric Ricker	0.50	0.24
30		Symmetric Ricker	0.25	0.32
31		Symmetric Ricker	0.25	0.64
32	3 Hz Long Base	Antisymmetric Ricker	0.50	0.16
33		Antisymmetric Ricker	0.50	0.22
34		Antisymmetric Ricker	0.25	0.44
35		Symmetric Ricker	0.50	0.16
36		Symmetric Ricker	0.50	0.24
37		Symmetric Ricker	0.50	0.32
38		Symmetric Ricker	0.25	0.64
39	3 Hz Short Base	Antisymmetric Ricker	0.50	0.10
40		Antisymmetric Ricker	0.50	0.16
41		Antisymmetric Ricker	0.50	0.22
42		Antisymmetric Ricker	0.25	0.44
43		Symmetric Ricker	0.50	0.08
44		Symmetric Ricker	0.50	0.16
45		Symmetric Ricker	0.50	0.24
46		Symmetric Ricker	0.25	0.32
47		Symmetric Ricker	0.25	0.64
48	4 Hz Long Base	Antisymmetric Ricker	0.50	0.22
49		Antisymmetric Ricker	0.25	0.44
50		Symmetric Ricker	0.50	0.24
51		Symmetric Ricker	0.50	0.32
52		Symmetric Ricker	0.25	0.64
53	4 Hz Short Base	Antisymmetric Ricker	1.00	0.10
54		Antisymmetric Ricker	0.50	0.10
55		Antisymmetric Ricker	0.50	0.16
56		Antisymmetric Ricker	0.50	0.22
57		Antisymmetric Ricker	0.25	0.16
58		Antisymmetric Ricker	0.25	0.22

(Continues)

DOI: 10.1002/eqe

Table III. (Continued)

No.	Specimen configuration	Excitation type	T_p [s]	a_p [g]
59		Antisymmetric Ricker	0.25	0.44
60		Symmetric Ricker	0.50	0.16
61		Symmetric Ricker	0.50	0.24
62		Symmetric Ricker	0.25	0.16
63		Symmetric Ricker	0.25	0.32
64		Symmetric Ricker	0.25	0.64

- *Asymmetry of the response*: An eccentricity of the center of gravity of the top mass with respect to the center of the specimen base plate along the horizontal x-axis in the plane of rocking results in longer rocking half cycles and larger rocking angle amplitudes in the direction of the eccentricity. Specimen eccentricity might occur because of the specimen geometry imperfections (the threaded holes in the base plate are not perfectly centered or perfectly perpendicular to the base plate bottom surface, the holes in the top weight are not perfectly centered) and because of possible plastic deformations of the column. In Figure 3 (left), the x-direction position of marker 3 (Figure 1, right) is compared to the average value of the x-direction position of markers 1 and 2. The measurements were taken before the start of each test. Four out of the eight specimens have a negligible eccentricity of the top weight. The 10 mm eccentricity of the 4 Hz Long Base specimen is, however, large. An extra 1 kg weight was added on the top of this specimen to compensate for this large eccentricity. The geometric eccentricity measurements remain virtually the same for repeated tests with the same specimen. Hence, the columns did not deform plastically during any of the tests.
- *Sliding*: There was practically no sliding for the tests with short base specimens (Figure 3, middle). For the long base specimen tests, maximum sliding was 1.7 mm.
- *Stepping and twisting*: The maximum base plate rotation around the y-axis observed during a test was taken as a measure of stepping (Figure 3, right). The measured twist angle was less than 0.4° in a majority of the tests, which was considered to be small and an indication that there was no stepping. Similar to the observations made for the sliding measurement, stepping was more prominent for the long base specimens.

3.1. General observations

Indicative measured response time histories of the normalized base rotation θ/α and the normalized elastic column deformation u/u_{cr} (where u_{cr} is defined in equation (25) of [9]) for the selected specimens are plotted in Figures 4 and 5. The response obtained using the analytical model developed in the companion paper [9] is also shown. The following was observed during the tests:

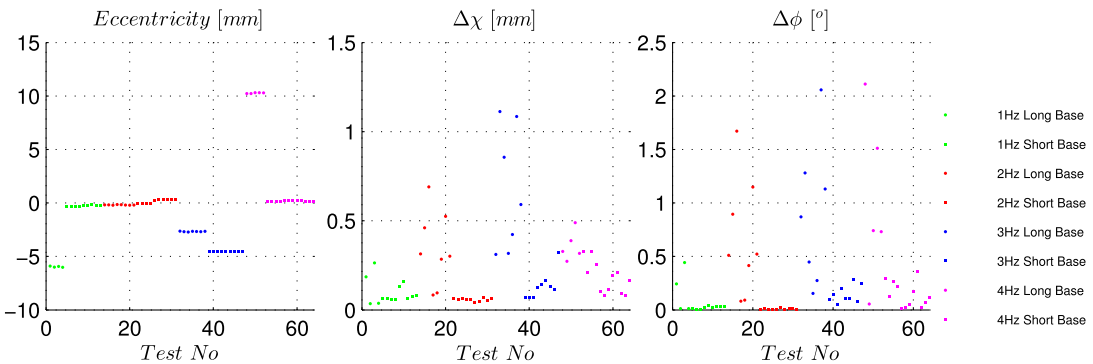

Figure 3. Eccentricity of the top weight with respect to the center of the base (left); measured sliding displacement (middle); and measured twist about the vertical axis (right).

DOI: 10.1002/eqe

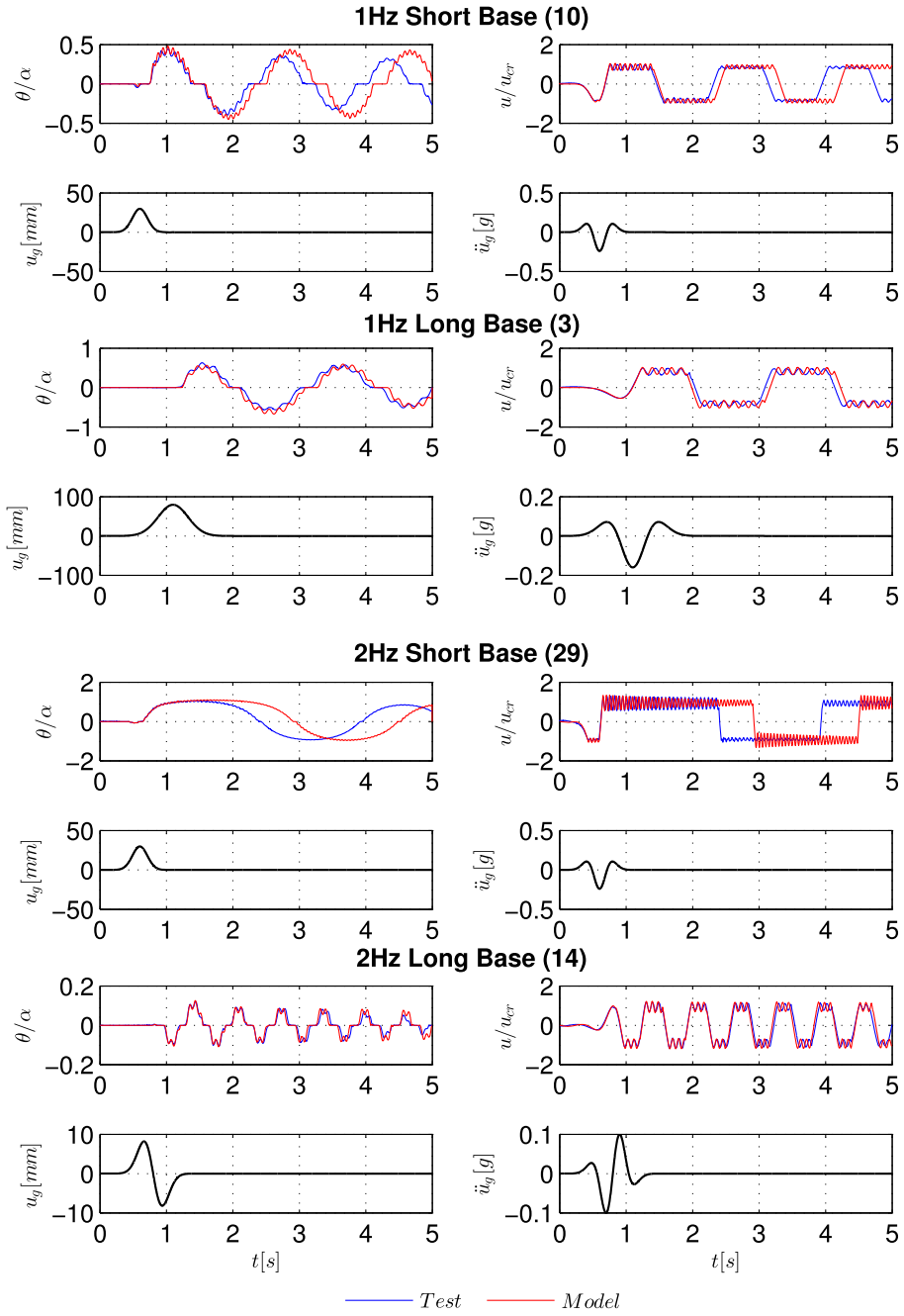

Figure 4. Indicative response time histories of the selected 1 Hz and 2 Hz specimens enumerated per Table III.

- The influence of the column elastic deformations on the rocking angle is clear in the 1 Hz Short Base and the 2 Hz Long Base tests. For the test with the 4 Hz Short Base specimen, this influence is minor, and the rocking angle time history is smooth;
- The elastic column oscillates with high frequency about an average displaced position. This average displacement changes sign with every impact;
- The duration of the full contact phase upon impact decreases with an increase of the specimen frequency;
- No damping is apparent in the uplifted oscillations of the 1 Hz Short Base and Long Base specimens and the 2 Hz Long Base specimen;

DOI: 10.1002/eqe

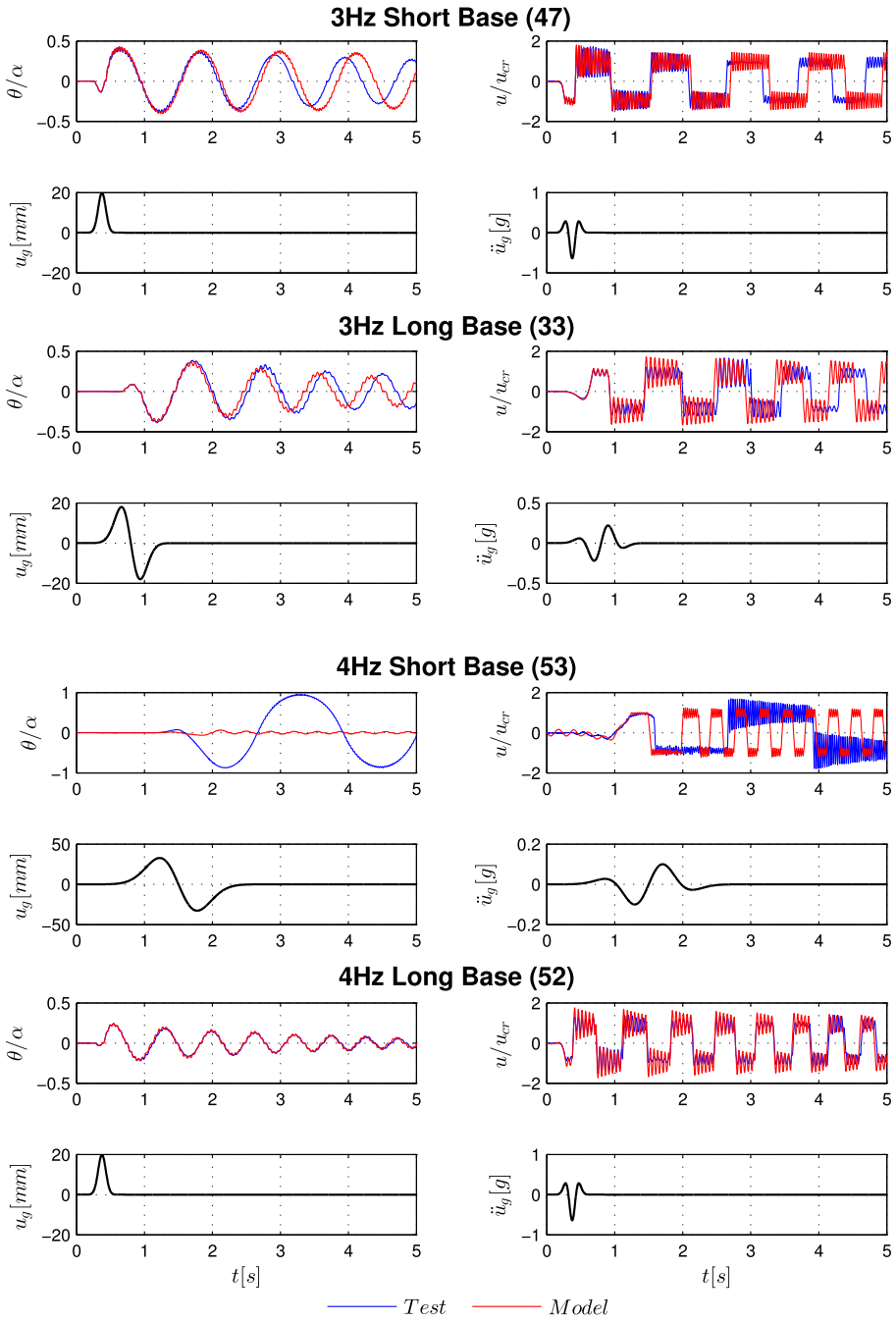

Figure 5. Indicative response time histories of the selected 3 Hz and 4 Hz specimens enumerated per Table III.

- The 'back and forth' motion discussed in Figure 3 of [14] was not observed in any of the conducted tests.

Figure 6 plots the response recorded during Test 41 (Specimen 3 Hz Short Base). The elastic deformation time history is irregular. The amplitude of the uplifted oscillations is different for every rocking half-cycle. Furthermore, the elastic deformation increases during the first rocking half-cycle, making the apparent damping negative. In order to find out if these irregularities are reproducible, the test was repeated. The time history of the second test is shown in red in Figure 6. In the second

DOI: 10.1002/eqe

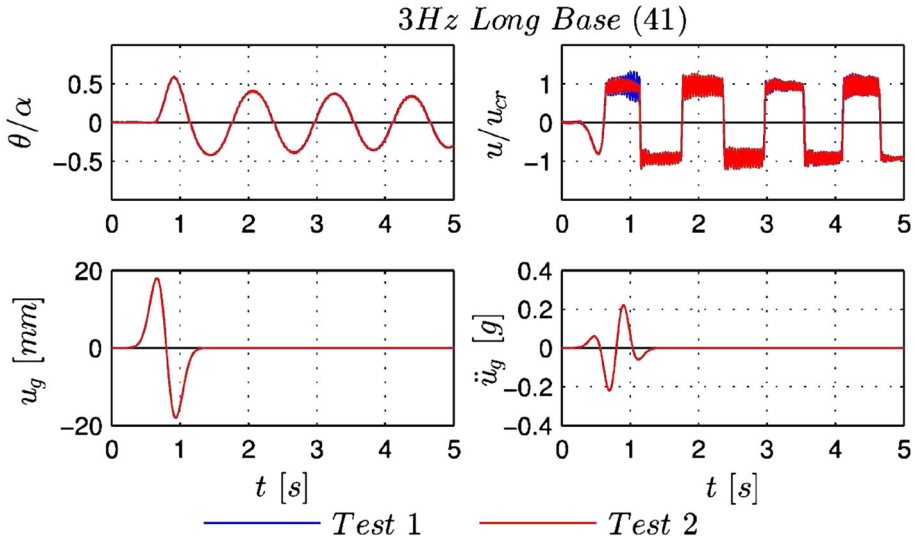

Figure 6. Test 41 performed twice.

run, there was no apparent negative damping and the amplitudes of the first few half-cycles differ only slightly. It is, however, interesting to note that the elastic column deformation response time history for the last few rocking-cycles of the second run precisely matches that recorded during the first run. Repeatability of the test results shows that these response irregularities are not random. They might occur because of higher mode vibration of the column or due imperfections of the specimens, both leading to more complicated motion of the specimen.

4. COMPARISON BETWEEN EXPERIMENTAL AND ANALYTICAL RESULTS

Two analytical models for computing the rocking response of deformable cantilever structures presented in [9] are considered. Two energy dissipated at impact is modeled by either the ADJex model (derived from that proposed by Acikgoz and DeJong [14]) or the Vertical Velocity Energy Loss (VVEL) model proposed in [9]. The responses computed using the two models for energy dissipated at impact are compared to the data obtained from experiments described above with three objectives: (i) to validate the models; (ii) to adjust the damping ratio used in the analytical models to better match the observed damping; and (iii) to compare the models and evaluate their accuracy and precision.

4.1. Energy dissipation at impact

Although not an ideal measure, reduction of the rocking angle amplitude is used as a measure of the energy dissipated at impact. This is because the velocities of the specimen masses could not be measured with sufficient accuracy without modifying the specimen masses using heavy velocity measuring instruments. Referring to Figure 7, the rocking amplitude ratio r_A is defined as follows:

$$r_A = \frac{A_{i+2}}{A_i} \tag{1}$$

where i is the number of half-cycles. The amplitude ratio is taken over two half-cycles in order to eliminate the influence of specimen eccentricity. This measure is expected to reflect the energy loss during impact when the elastic deformation is small (i.e. for stiffer specimens, for more slender

DOI: 10.1002/eqe

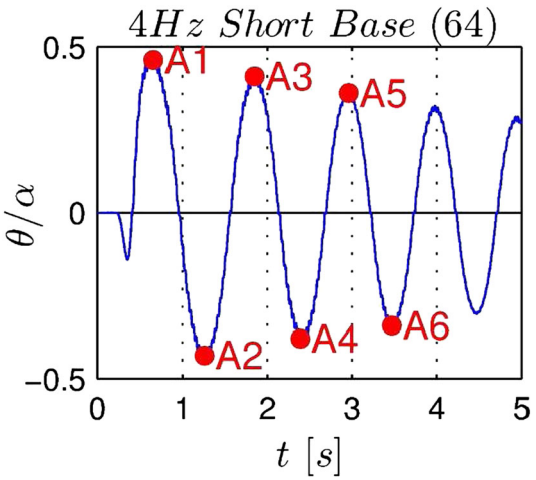

Figure 7. Amplitudes of rocking half-cycles in Test 64.

specimens and for larger rotation angles, θ). A measure of rocking amplitude decay because of energy dissipation at impact (*MoAD*) is defined as:

$$MoAD = 1 - r_{\mathrm{A}}. \tag{2}$$

A ratio of the values of *MoAD* computed using the analytical models over the experimentally determined *MoAD* value is defined as:

$$r_{MoAD} = \frac{MoAD_{theo}}{MoAD_{\mathrm{exp}}} \tag{3}$$

to compare the models. A r_{MoAD} value larger than 1 indicates that the analytical model dissipates more energy than measured in the corresponding test. Only the 64 tests with a reasonably large rocking angle (Table III) are considered.

The median and median absolute deviation (MAD) values of r_{MoAD} values for the considered 64 tests are computed and listed in Table IV. The MAD is the median of the absolute deviations from the data's median:

$$MAD = median_i\left(\left|X_i - median_j\left(X_j\right)\right|\right) \tag{4}$$

where $median_k(X_k)$ denotes the sample medial of $\{X_1, \ldots, X_n\}$. It indicates the dispersion of the data, but is less sensitive to outliers than the standard deviation. Because the number of tests with the short base is larger than the number of tests with the long base (Table III), the statistics are separated. The ADJex energy dissipation at impact model overestimates the energy dissipated at impact for both base plate sizes, while the VVEL model accurately predicts the energy dissipated at impact for long base specimens, but it underestimates it for short base specimens. Thus, the VVEL model predicts larger rotations, making it more conservative than the ADJex model with respect to this design variable. A comparison of the *MAD* values indicates that the VVEL model is more precise than the ADJex

Table IV. Median and MAD of the amplitude decay ratio r_{MoAD} for the ADJex and the VVEL models [9].

	All tests		Long base tests only		Short base tests only	
Analytical model	Median	MAD	Median	MAD	Median	MAD
ADJex	1.487	0.890	2.040	1.706	1.380	0.465
VVEL	0.630	0.435	1.059	0.562	0.507	0.194

DOI: 10.1002/eqe

model. Note, however, that the precision of the VVEL model predictions is still relatively low for the long base tests compared to a fairly high prediction precision for the short base tests.

The rocking angle response time history is shown in Figure 8 to further demonstrate the differences between the two energy dissipation models. For the 2 Hz Long Base specimen, shown on the left, energy dissipation at impact and subsequent rotation are accurately predicted by the VVEL model for the first few rocking cycles and then they are underestimated. The ADJex models overestimates the energy dissipated and the rotation at all impacts. For the 1 Hz Short Base specimen, shown on the right, the ADJex model overestimates the energy dissipation while the VVEL model underestimates it. Plot 8 (bottom) shows a detail of the response time histories. It can be clearly seen that the ADJex model predicts a 'back and forth' double impact, which is not experimentally observed. This is a source of extra damping and the reason why the ADJex model is not considered further. Note, however, that a 'bouncing back' double impact observed in the experiment is not predicted by any model.

4.2. *Uplifted frequency and damping ratio*

Figure 9 plots the measured uplifted frequencies (left) and compares them to the ones predicted by the analytical model (equation (18) of [9]). The values of the frequency ratios (right) range from a minimum of 0.73 for the 1 Hz Short Base specimen to a maximum of 1.04 for the 4 Hz Long Base specimen. The frequency ratios increase and approach the desired value of 1 for the stiffer specimens. The ratios are slightly higher for the equally stiff specimens with a long base. These observations agree with those made during the free rocking vibration tests conducted using similar specimens in [15]. Therefore, the analytical deformable cantilever rocking model predicts the uplifted frequency reasonably accurately.

Figure 10 plots the measured uplifted damping ratio (left), the ratio of the measured uplifted damping ratio to the value predicted by equation (19) of [9] (middle) and the ratio of the measured uplifted over measured fixed-base damping ratio (right). Data from only 13 out of 64 tests (Table III) are plotted because only these tests had a sufficient number of oscillations with monotonically decreasing amplitude to calculate the damping ratios. It is evident that the theoretically predicted [16] increase of damping ratio in the uplifted state of the specimens is not observed experimentally. In fact, the measured uplifted damping ratio is of the same order of magnitude as the fixed-base damping ratio. This contradicts theoretical derivations [14, 16, 17] that predict a significant increase of damping for vibration s in the uplifted configuration. Furthermore, in many cases, measured damping ratio in the uplifted configuration decreased during oscillations. This is in agreement with

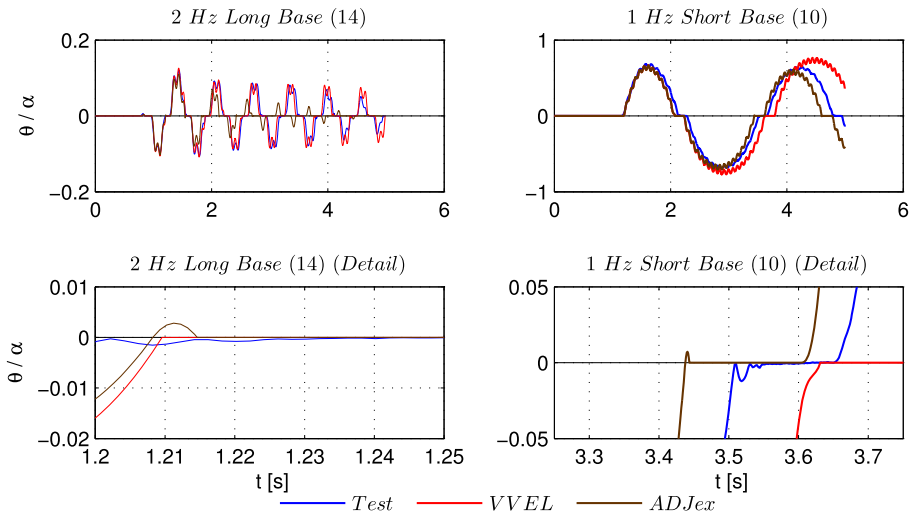

Figure 8. Comparison of the time history response of ADJex and VVEL models [9] to the measured test data. The numbering of the specimens follows Table III.

DOI: 10.1002/eqe

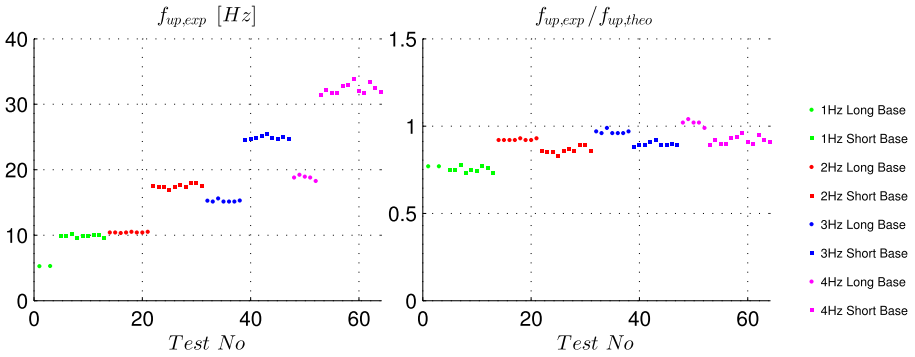

Figure 9. Measured uplifted frequency (left) and ratio of the measured uplifted frequency over the uplifted frequency predicted by the model [9] (right).

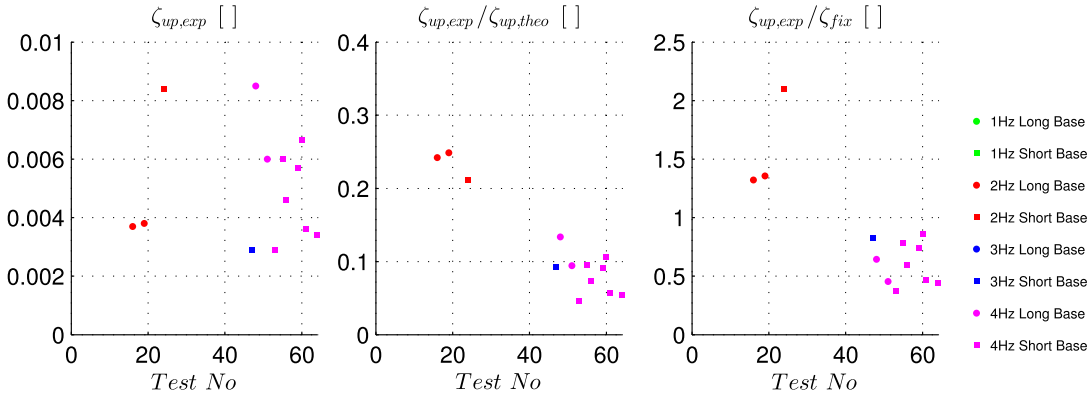

Figure 10. Measured uplifted damping ratio (left), ratio of the measured uplifted damping ratio over the uplifted damping ratio predicted by the model [9] (middle) and ratio of the measured uplifted damping ratio over the measured fixed-base damping ratio (right).

the observations made in free rocking vibration tests [15]. For this reason, the damping ratio in the analytical model [9] was adjusted as follows: the experimentally measured fixed-base damping ratio is divided by the square-root term in equation (19) of [9]. As a consequence, the uplifted damping ratio in the analytical model will be equal to the measured fixed-base damping ratio.

4.3. Time history of rocking response

The response time history comparisons shown in Figures 4 and 5 are made using the VVEL model [9] for energy dissipated at impact with the reduced uplifted damping ratio. Explaining the observed response rests on the relation between the natural vibration period of the structure and the amplitude of its motion. The vibration period of linear-elastic structures (e.g. fixed-base linear elastic cantilevers) does not depend on the amplitude of the oscillations. Vibration of structures characterized by a bi-linear force-deformation response with hardening (a positive post-yield stiffness) can be characterized by an effective period measure [18, 19] that depends, but not strongly, on the amplitude of the oscillations. However, the vibration period of rocking systems characterized by a rigid-softening (negative post-yield stiffness) behavior depends strongly on the amplitude of motion [20]. The apparent period of oscillatory motion of a rocking, but not overturning, rigid block increases at an increasing rate as the amplitude of motion approached the critical overturning (instability) rotation angle (Figure 2 of [21]). The problem of correctly predicting the rocking time history is further compounded by the fact that errors in amplitude prediction lead to errors in phase prediction. The errors grow with the increasing magnitude of

DOI: 10.1002/eqe

motion. This is why small amplitude rocking rotations are predicted more accurately than the large ones that occur when the rocking structure is close to overturning (Figure 4, test 29).

In Test 53 (Figure 5), the model fails to capture the normalized rotation θ/α time history. While the model predicts only a minor uplift, the rocking angle amplitude measured in the test was close to the specimen slenderness α; thus, the specimen was close to overturning. This large difference between the model prediction and the experiment results occurred, in large part, because the excitation used, an antisymmetric Ricker wavelet with $T_p = 1.0\,\mathrm{s}$ and $a_p = 0.10\,\mathrm{g}$, places the tested specimen in a very sensitive part of the rocking spectrum, where a small difference in the acceleration amplitude can lead to a big difference in the rocking angle. This will be discussed further. Another significant source of error in predicting the normalized rotation time history θ/α is the model for energy losses because of impact. The VVEL model, adopted here, fits the test results for the long base specimens well, but underestimates the test results for short base specimens. This is the reason why the time histories of θ/α are generally more accurately predicted for the long base specimens.

4.4. *Maximum rocking angle and column relative displacement*

The rocking structures response parameters most relevant for design are: (i) the maximum rocking angle, used to assess the likelihood of an overturning failure; and (ii) the maximum relative displacement of the top of the cantilever with respect to the base plate, used to determine the internal forces in the column. Figure 11 (left) plots the ratio of the maximum rocking angle measured in the tests over the one computed using the VVEL model. The predictions are generally accurate. For most tests, the difference between measured and the predicted results is less than 10%. The largest outlier is the data from Test 53, where the experiment/prediction ratio is 14.4 (not shown in plot). The time history for this test is shown in Figure 5. This test is further discussed in a later section.

Figure 11 (middle) plots the ratio of the maximum relative column displacement measured in the tests over the one computed using the model. The model prediction is relatively good: the error is larger than 25% in only one test, Test 53. The model is conservative for 60 out of the 64 considered analytical pulse tests.

Figure 11 (right) compares the measured and predicted average relative displacement in the uplifted state. The model prediction is very accurate and precise (the spread is very small).

4.5. *Rocking spectra for analytical pulse excitations*

A rocking spectrum for analytical pulse excitation plots the values of the maximum rotation angle θ normalized by the slenderness angle α of the deformable rocking structure in the space of the two normalized excitation parameters: the frequency parameter, a ratio of the analytical pulse frequency ω_p over the rocking time constant parameter p and the amplitude parameter, a ratio of the analytical pulse amplitude a_p over gtanα (g is the acceleration of gravity). The outcomes of a rocking test are

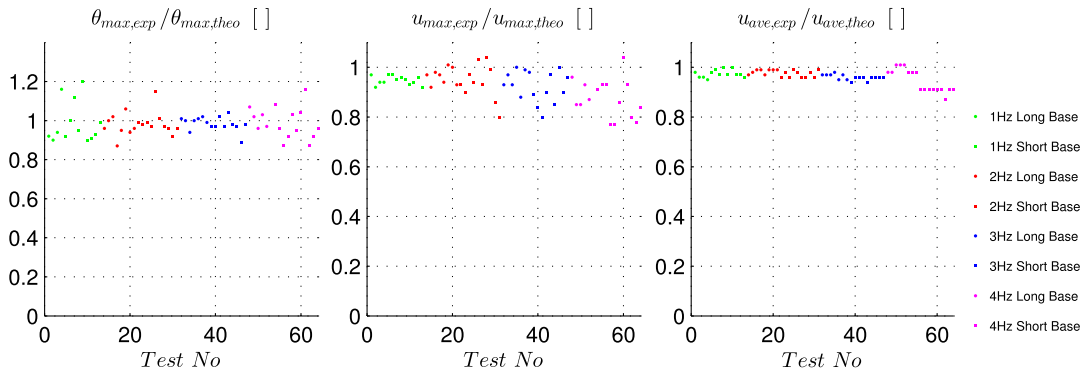

Figure 11. Comparison of the maximum base rotation angle (left), the maximum relative displacement (middle) and the average relative displacement (right).

DOI: 10.1002/eqe

represented by the magnitude of the normalized rotation angle as follows: (i) no uplift: $\theta/\alpha = 0$; (ii) rocking without overturning; (iii) overturning in the positive direction; and (iv) overturning in the negative direction.

The rocking spectra for the 1 Hz Short Base specimen for an antisymmetric Ricker wavelet excitation and the 4 Hz Short Base specimen for a symmetric Ricker wavelet excitation are plotted in Figure 12. Tests differing in the applied excitation (Table III) are indicated by 'plus' signs. An

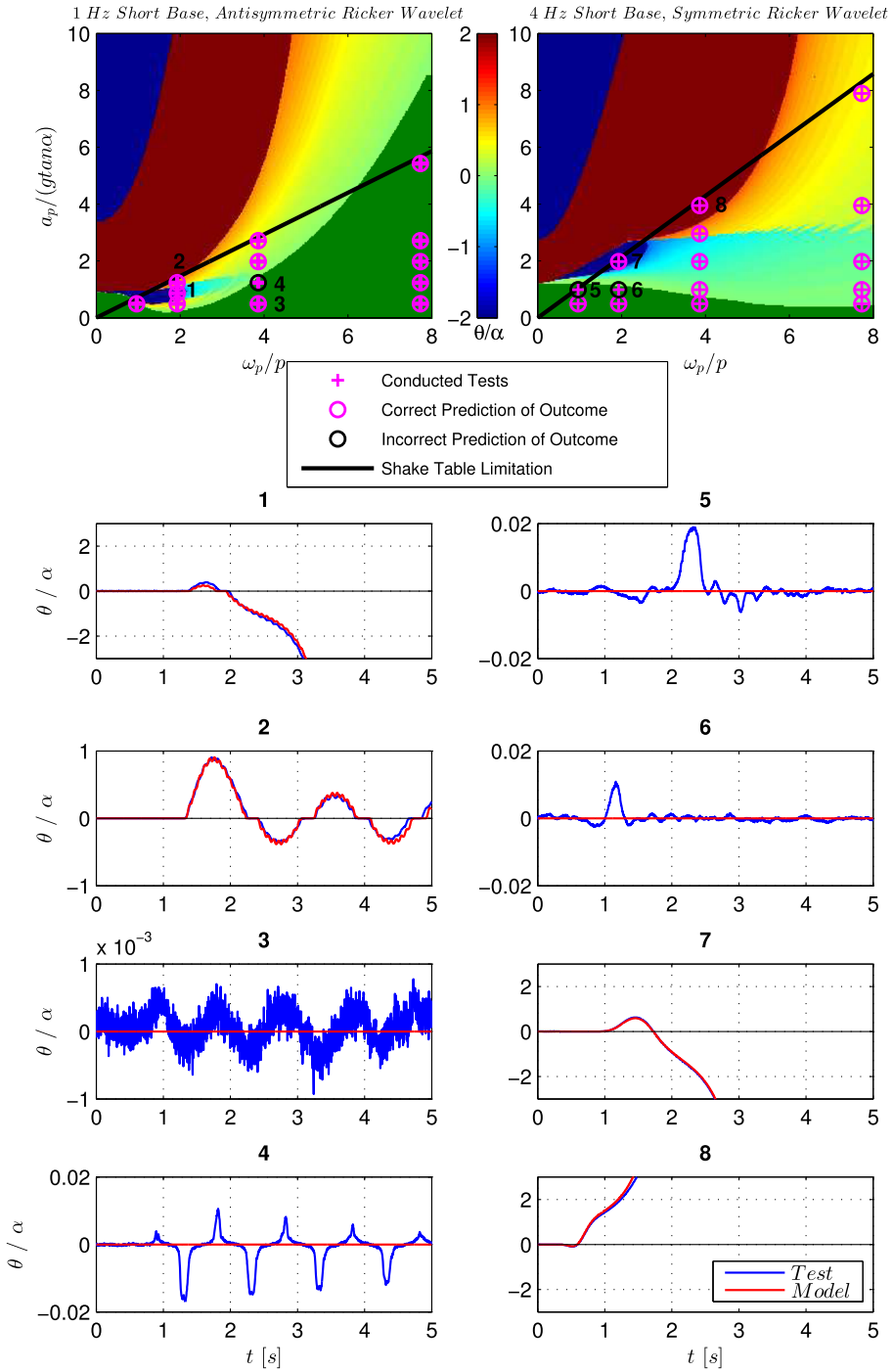

Figure 12. Rocking spectra for the 1 Hz Short Base specimen under antisymmetric Ricker wavelet excitation and for the 4 Hz Short Base specimen under symmetric Ricker wavelet excitation; normalized rocking rotation angle response time histories for the indicated tests.

DOI: 10.1002/eqe

additional test was conducted for the 1 Hz Short Base specimen in order to examine the overturning zone between the two rocking-without-overturning zones in the rocking spectrum. The coordinates for this test, labeled as point 1 in Figure 12, are $\omega_p/p = 1.9$ and $a_p/(g\tan\alpha) = 0.9$.

Uplifts of the base were measured in all tests. For example, point 3 in Figure 12 shows a test where the measured maximum rocking angle was equal to about 0.0006α (as seen in the normalized rotation angle time history for this test shown in Figure 12), corresponding to the base plate edge uplift of about 0.007 mm. Compared to the 0.6 mm thickness of the sandpaper placed under the specimen, this uplift is small and may represent the deformation of the sandpaper layer itself. Therefore, a minimum rocking rotation angle amplitude threshold was chosen to identify the uplift event. This threshold was set at

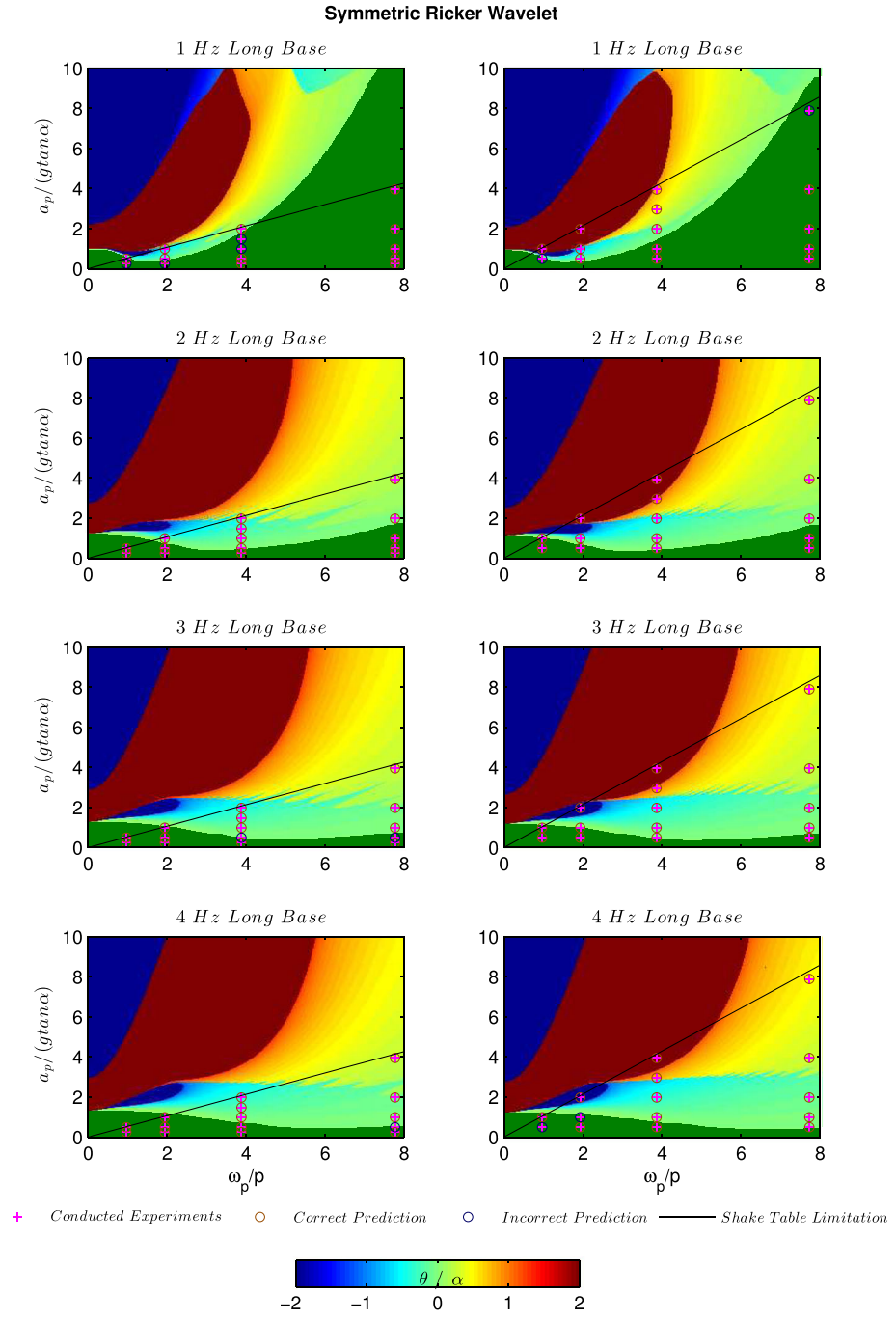

Figure 13. Rocking spectra for all specimen configurations for symmetric Ricker wavelet excitations.

DOI: 10.1002/eqe

0.01α for the short base specimens and at 0.0025α for the long base specimens. These values are equivalent to the base plate edge being 0.12 mm (one fifth of the sandpaper thickness) above the surface. With this definition of uplift, the specimen is considered to not have uplifted in the test 3 in Figure 12 (left). Therefore, the analytical model correctly predicted the outcome of this test.

A test point in Figure 12 is circled with a light circle if the outcome of the test was predicted correctly, and by a dark circle if the outcome was predicted incorrectly. Only one out of 13 tests was predicted incorrectly for the 1 Hz Short Base specimen, while only two of 15 tests were

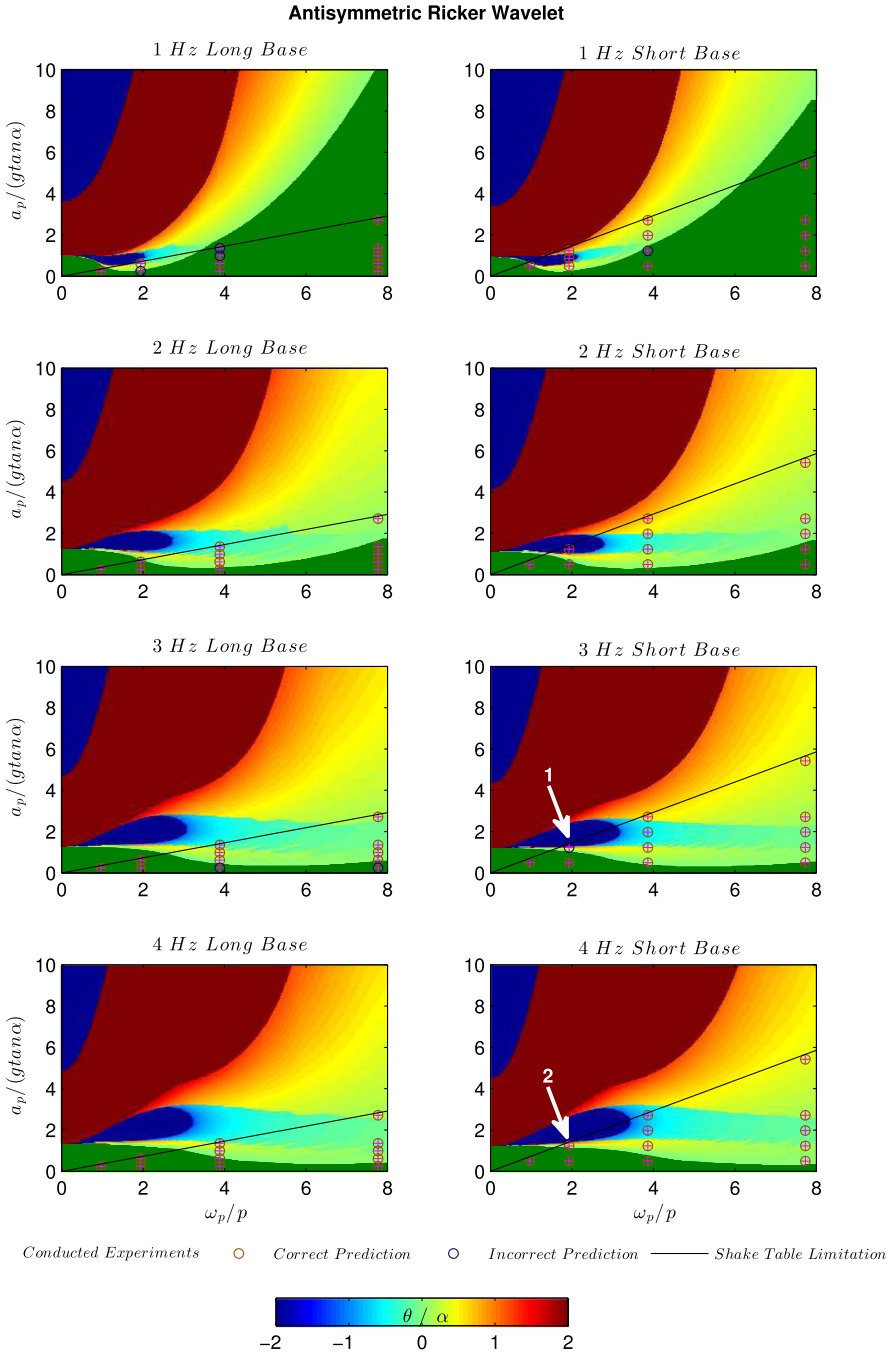

Figure 14. Rocking spectra for all specimen configurations for antisymmetric Ricker wavelet excitations. The time histories of the normalized rotation angle response for the 3 Hz Short Base and 4 Hz Short Base tests are shown in Figure 15.

DOI: 10.1002/eqe

predicted incorrectly for the 4 Hz Short Base specimen. Representative normalized rocking rotation angle response time histories recorded during the tests and predicted using the VVEL model for the specimens identified by points 1 through 8 in the spectra in Figure 12 are also shown. The rest of the plots of Figure 12 show time histories of the response of indicative tests. Overturning was correctly predicted for tests shown by points 1, 7 and 8, including the direction of overturning. Rocking response was predicted very well for the test marked by point 2, but was not predicted to occur for tests at points 4, 5 and 6.

The rocking spectra for all specimen configurations are summarized in Figure 13 for the symmetric and in Figure 14 for the antisymmetric Ricker wavelet excitations. The model predicts the outcome of the experiments quite well, with only 20 out of 217 experiments predicted incorrectly. Uplift and rocking of the specimens were observed during 19 out of these 20 incorrect predictions. However, the measured uplift was very small, with the edge of the base plate never lifting more than 1 mm above the specimen base.

Specimen overturning was predicted correctly in all tests but one. Overturning of the 3 Hz Short Base specimen subjected to an antisymmetric Ricker wavelet excitation in one test was not predicted. The time history of the rocking angle for this test is shown in Figure 15 (left) where it is evident that the model barely avoids overturning. This is also confirmed in the rocking spectrum, where this test is close to the dark blue area of overturning in negative θ-direction. This test is in an area of the rocking spectrum that is very sensitive to changes of the acceleration amplitude a_p. For long excitation periods T_p (i.e. smaller values of the normalized frequency parameter ω_p/p) the test outcome can transition from no uplift to overturning with only a minor change of the acceleration

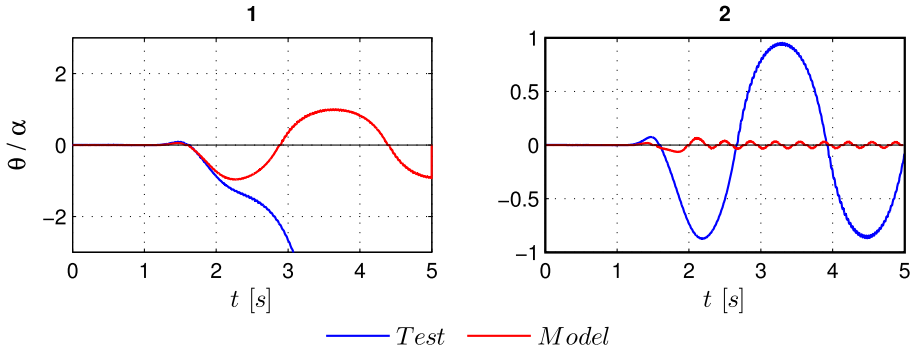

Figure 15. Time history the normalized rotation angle response for tests 1 and 2 indicated in Figure 14.

Table V. Tests with recorded ground motion excitations and rocking angle amplitudes larger than 0.05 α.

No.	Specimen configuration	Earthquake record
1	1 Hz Long Base	San Fernando, 1971
2		Erzican, 1992
3	1 Hz Short Base	San Fernando, 1971
4		Erzican, 1992
5		Aigion, 1995
6	2 Hz Long Base	San Fernando, 1971
7		Aigion, 1995
8	2 Hz Short Base	San Fernando, 1971
9		Erzican, 1992
10		Aigion, 1995
11	3 Hz Long Base	Aigion, 1995
12	3 Hz Short Base	San Fernando, 1971
13		Erzican, 1992
14		Aigion, 1995
15	4 Hz Long Base	Aigion, 1995
16	4 Hz Short Base	San Fernando, 1971
17		Erzican, 1992
18		Aigion, 1995

DOI: 10.1002/eqe

amplitude. That is the reason why the model fails to capture the experimental response. This sensitivity is confirmed in Figure 15 (right), where the time history comparison for the previously mentioned Test 53 is plotted. The specimen is close to overturning in the test, while model predicts only a minor uplift.

5. RESPONSE TO RECORDED GROUND MOTIONS

The response time histories recorded in tests where the specimens were excited using recorded ground motions listed in Table III are compared to the predictions obtained using the model. The conducted tests during which the measured amplitude of the rocking angle exceeded 0.05α are enumerated in

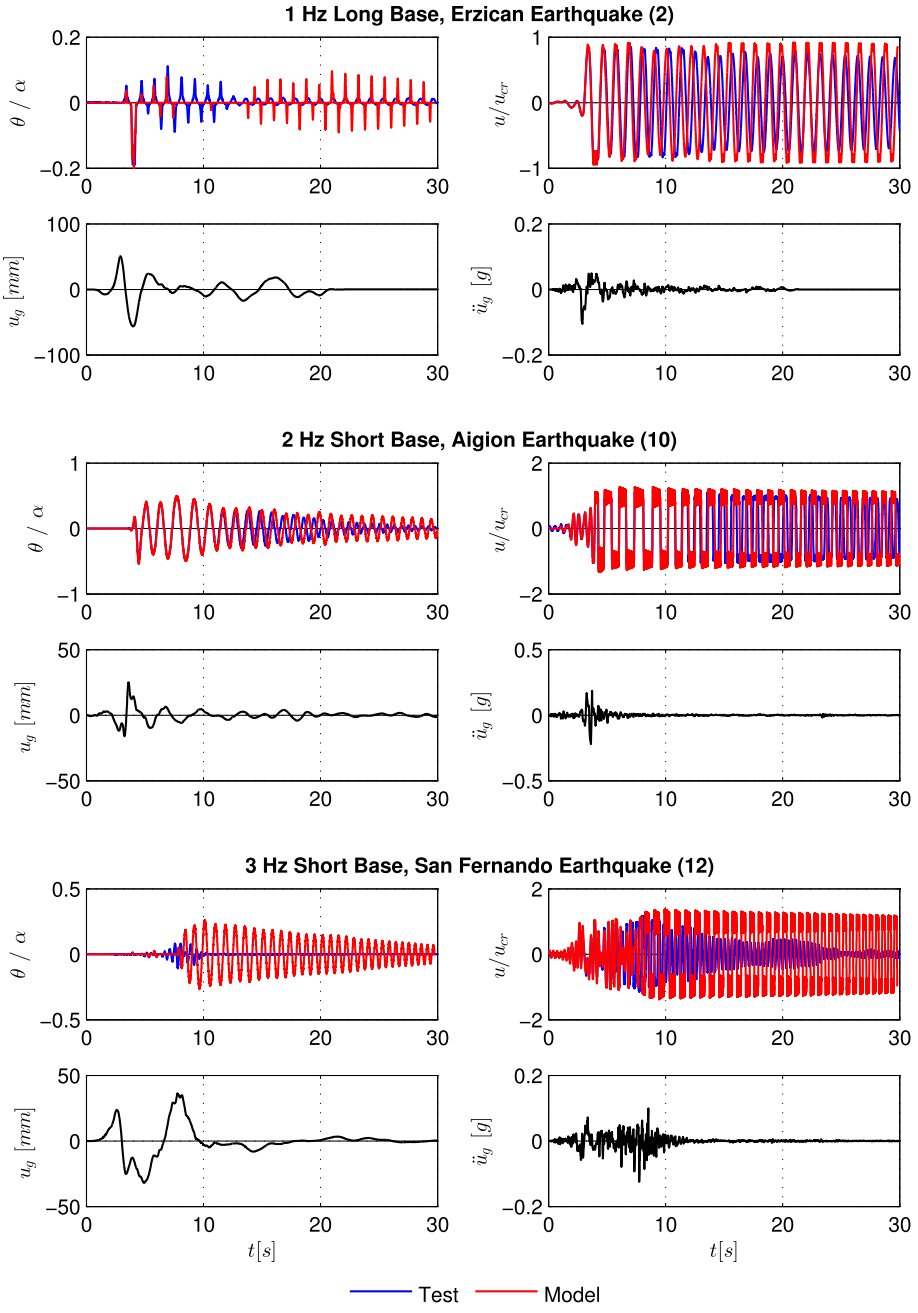

Figure 16. Indicative response time histories for the scaled recorded ground motion excitations. The test numbering follows that in Table V.

DOI: 10.1002/eqe

Table V. The responses in the indicative tests 2, 10 and 12 are shown in Figure 16, while the remaining test outcomes are detailed in [15].

5.1. Time history of rocking response

The match between the measure response time histories and those obtained from the model is, in general, much worse for the earthquake records compared to the Ricker wavelets. The prediction of the rocking angle for the 1 Hz Long Base specimens (test 2 in Table V) is inaccurate, especially in the second half of the shown response time history. Nevertheless, the maximum amplitude of the rocking angle, which occurs during the dominant acceleration pulse in the ground motion, is predicted accurately.

Interestingly, the phase of the rocking cycles is predicted correctly even towards the end of the time history shown, despite the difference in the rocking angle amplitudes. Also, there is a reasonably good match between the measured and the predicted elastic oscillation without uplift portion of the response, despite the differences in the rocking angle time history.

The rocking angle response time history is matched very well for test No. 10 (with the 2 Hz Short Base specimen and the 1995 Aigion Earthquake excitation). Only in the second half of the time history, when the accelerations are very small, does the model slightly overestimate the rocking angle. This can be attributed to the underestimate of the energy dissipated at impact for short base specimens that occurs in the VVEL model and is discussed in the companion paper [9]. The average relative column displacement is predicted correctly, while the amplitude of the uplifted oscillations is generally overestimated.

The prediction of the response of test No. 12 with the 3 Hz Short Base specimen and the 1971 San Fernando earthquake excitation was the worst among the tests listed in Table V. The estimate of the maximum rocking angle amplitude is off by a factor of 2.5. The time histories do not match. This test shows that an accurate prediction of the first major uplift is very important for a good match in the entire time history.

5.2. Maximum rocking angle and relative column displacement

The ratio of the maximum rocking angle measured in the tests over the maximum rocking angle predicted by the model is shown in Figure 17 (left) for the tests with recorded ground motion excitations. The ratio is 1 for tests 3 and 4 where overturning was predicted correctly. For most tests where the specimens rocked but did not overturn, the rocking rotation angle amplitude is predicted accurately. Nevertheless, there are outliers with ratios over 2 or under 0.5. The predictions of the rocking angle amplitude were the best for the 1995 Aigion earthquake and the worst for the 1971 San Fernando earthquake records. The comparison for the maximum relative column displacement test and prediction data is plotted in Figure 17 (right). The prediction is accurate for the majority of the tests, with the outliers being much less extreme than for the maximum base rotation. The maximum base rotation response to recorded ground motions was predicted with an error smaller than 30% in 14 out of the 17 cases. The maximum elastic displacement of the column was predicted with an error smaller than 30% in 17 out of the 17 cases.

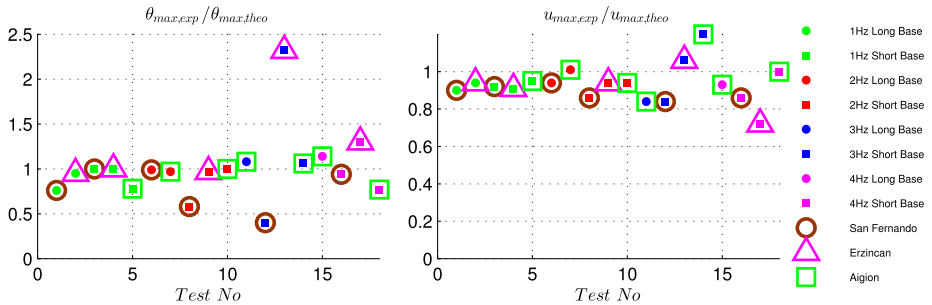

Figure 17. Comparison of maximum rocking angle (left) and maximum relative column displacement (right) for the tests with earthquake excitations.

DOI: 10.1002/eqe

6. CONCLUSIONS

The use of rocking as a seismic response modification technique for deformable cantilever structures is hindered by the lack of a verified and validated analytical model. A series of experiments were performed to validate analytical models for rocking of deformable cantilever structures with massive columns and concentrated masses at the base and the top of the cantilever developed in a companion paper [9]. Specimens with four different fundamental vibration frequencies, mounted on two different uplifting bases, were excited by analytical pulses and real ground motions using a shaking table. A total of 240 tests were conducted.

Two analytical models for computing the energy dissipated at impact during rocking response of deformable cantilever structures presented in [9] are the ADJex model (a modified model proposed by Acikgoz and DeJong [14]) and the Vertical Velocity Energy Loss (VVEL) model. Both models were verified. During the validation process (comparison of model predictions and measured data) the ADJex model was found to be less conservative than the VVEL model.

The increase of viscous damping during flexural vibrations of the column in the uplifted configuration proposed in [16] and adopted in [14, 17] was not experimentally observed. Instead, a very small damping value (smaller than the fixed base damping value, but consistent with experimental observations) was adopted. This result challenges the 'increased viscous damping during rocking' assumption of all previous related studies.

The agreement between the measured and the computed responses for sinusoid pulse excitations was very good, considering the highly non-linear nature of the problem, high sensitivity of the rocking outcomes to the amplitude of excitation in some regions of the rocking spectrum and the challenges of conducting the tests. The model predicted the uplifted frequency, the rocking angle and the uplifted average elastic displacement for recorder ground motions with errors smaller than 30%.

Based on the outcomes of the verification and validation process presented in this paper, the model with the VVEL impact energy dissipation assumption can be recommended for simulation of the response of deformable cantilever columns to analytical and recorded ground motions. There is, however, room for refinement, particularly with respect to modeling the energy dissipated at impact and the damping of oscillations in the uplifted state. The test data [10] used in this paper can be used to verify and validate the improved models for uplifting and rocking response of deformable cantilever structures with concentrated and distributed masses.

REFERENCES

1. Lipscombe, PR, Pellegrino, S. Free rocking of prismatic blocks. *Journal of Engineering Mechanics* 1993; **119**(7):1387–1410.
2. Peña F, Prieto F, Lourenço PB, Campos Costa A, Lemos JV. On the dynamics of rocking motion of single rigid-block structures. *Earthquake Engineering and Structural Dynamics* 2007; **36**(15):2383–2399.
3. Ma QT, Khan MH. Free vibration tests of a scale model of the South Rangitikei Railway Bridge. In *Proceedings of the New Zealand Society for Earthquake Engineering Annual Conference*, *Engineering an Earthquake Resilient NZ*, 2008.
4. Konstantinidis D, Makris N. Experimental and analytical studies on the response of 1/4-scale models of freestanding laboratory equipment subjected to strong earthquake shaking. *Bulletin of Earthquake Engineering* 2010; **8**(6):1457–1477.
5. Ma QTM. The mechanics of rocking structures subjected to ground motion (Doctoral dissertation, ResearchSpace@ Auckland) 2010.
6. ElGawady MA, Ma Q, Butterworth JW, Ingham J. Effects of interface material on the performance of free rocking blocks. *Earthquake Engineering and Structural Dynamics* 2011; **40**(4):375–392.
7. Baratta A, Corbi I, Corbi O. Towards a seismic worst scenario approach for rocking systems: analytical and experimental set-up for dynamic response. *Acta Mechanica* 2013; **224**(4):691–705.
8. Zhang H, Brogliato B, Liu C. Dynamics of planar rocking-blocks with Coulomb friction and unilateral constraints: comparisons between experimental and numerical data. *Multibody System Dynamics* 2014; **32**(1):1–25.
9. Vassiliou MF, Truniger R. Stojadinovic B. An analytical model of a deformable cantilever structure rocking on a rigid surface: development and verification. *Earthquake Engineering and Structural Dynamics* 2015.
10. Truniger R. Experimental investigation of the response of flexible rocking oscillators to ground shaking, Master Thesis—Spring Semester 2014, ETH Zürich—Institute of Structural Engineering, 2014

DOI: 10.1002/eqe

11. Bachmann H, Baumann M, Lestuzzi P, Wenk T. Der neue ETH-Erdbebensimulator, *Schweizer Ingenieur und Architekt SI + A*, Heft 4/99. Zürich; 1999
12. Ricker N. Further developments in the wavelet theory of seismogram structure. *Bulletin of the Seismological Society of America* 1943; **33**:197–228.
13. Vassiliou MF, Makris N. Analysis of the rocking response of rigid blocks standing free on a seismically isolated base. *Earthquake Engineering and Structural Dynamics* 2012; **41**(2):177–196.
14. Acikgoz S, DeJong MJ. The interaction of elasticity and rocking in flexible structures allowed to uplift. *Earthquake Engineering and Structural Dynamics* 2012; **41**(15):2177–2194.
15. Truniger R. Experimental investigation of rocking of elastic columns, Projektarbeit Master—Spring Semester 2013, ETH Zürich—Institute of Structural Engineering, 2013.
16. Chopra AK, Yim SCS. Simplified earthquake analysis of structures with foundation uplift. *Journal of Structural Engineering* 1985; **111**(4):906–930.
17. Oliveto G, Caliò I, Greco A. Large displacement behaviour of a structural model with foundation uplift under impulsive and earthquake excitations. *Earthquake Engineering and Structural Dynamics* 2003; **32**:369–393.
18. Makris N, Kampas G. Estimating the "effective period" of bilinear systems with linearization methods, wavelet and time-domain analyses: from inelastic displacements to modal identification. *Soil Dynamics and Earthquake Engineering* 2013; **45**:80–88.
19. Makris N, G Kampas. The engineering merit of the "effective period" of bilinear isolation systems. *Earthquakes and Structures* 2013; **4**(4):397–428.
20. Makris N, Konstantinidis D. The rocking spectrum and the limitations of practical design methodologies. *Earthquake Engineering and Structural Dynamics* 2003; **32**(2):265–289.
21. Housner GW. The behavior of inverted pendulum structures during earthquakes. *Bulletin of the Seismological Society of America* 1963; **53**(2):403–417.

DOI: 10.1002/eqe